

On the non-detection of solar-like pulsations in the host star GJ 504 observed by TESS

MARIA PIA DI MAURO,¹ RAFFAELE REDA,^{2,1} SAVITA MATHUR,^{3,4} RAFAEL A. GARCÍA,⁵ DEREK L. BUZASI,⁶ ENRICO CORSARO,⁷ OTHMAN BENOMAR,^{8,9}
LUCÍA GONZÁLEZ CUESTA,^{3,4} KEIVAN G. STASSUN,^{10,11} SERENA BENATTI,¹² VALENTINA D'ORAZI,^{13,14} LUCA GIOVANNELLI,^{2,1} DINO MESA,¹³ AND
NICOLAS NARDETTO¹⁵

¹INAF-IAPS, Istituto di Astrofisica e Planetologia Spaziali Via del Fosso del Cavaliere 100 00133 Roma, Italy

²Dipartimento di Fisica, Università di Roma Tor Vergata, Via della Ricerca Scientifica 1, 00133 Roma, Italy

³Instituto de Astrofísica de Canarias (IAC), 38205 La Laguna, Tenerife, Spain

⁴Universidad de La Laguna (ULL), Departamento de Astrofísica, E-38206 La Laguna, Tenerife, Spain

⁵AIM, CEA, CNRS, Université Paris-Saclay, Université de Paris, Sorbonne Paris Cité, F-91191 Gif-sur-Yvette, France

⁶Dept. of Chemistry & Physics, Florida Gulf Coast University, 10501 FGCU Blvd. S., Fort Myers, FL 33965 USA

⁷INAF-Astrophysical Observatory of Catania, Via S. Sofia 78 95123 Catania, Italy

⁸National Astronomical Observatory of Japan, Mitaka, Tokyo, Japan

⁹Center for Space Science, New York University Abu Dhabi, UAE

¹⁰Vanderbilt University, Department of Physics & Astronomy, 6301 Stevenson Center Ln., Nashville, TN 37235, USA

¹¹Vanderbilt Initiative in Data-intensive Astrophysics (VIDA), 6301 Stevenson Center Lane, Nashville, TN 37235, USA

¹²INAF - Osservatorio Astronomico di Palermo, Piazza del Parlamento 1, 90134 Palermo, Italy

¹³INAF Osservatorio Astronomico di Padova, vicolo dell'Osservatorio 5 35122, Padova Italy

¹⁴School of Physics and Astronomy, Monash University, Clayton, VIC 3800, Australia

¹⁵Université Côte d'Azur, Observatoire de la Côte d'Azur, CNRS, Laboratoire Lagrange, France

(Received; Accepted)

Submitted to ApJ

ABSTRACT

We present the results of the analysis of the photometric data collected in long-cadence mode by the Transiting Exoplanet Survey Satellite (TESS) for GJ 504, a well studied planet-hosting solar-like star, whose fundamental parameters have been largely debated during the last decade. Several attempts have been made by the present authors to isolate the oscillatory properties expected on this main-sequence star with mass $M = (1.28 \pm 0.07)M_{\odot}$, radius $R = (1.38 \pm 0.2)R_{\odot}$ and age ≤ 2.6 Gyr, as predicted by theoretical models. We found only a marginal hint of the presence of pulsations around $\approx 2000 \mu\text{Hz}$ and we report only with low statistical significance a large separation $\Delta\nu = (85.0 \pm 3.6)\mu\text{Hz}$. The suppression of the amplitude of the acoustic modes can be explained by the high level of magnetic activity revealed for this target, not only by the study of the photometric light-curve, but also by the analysis of three decades available of Mount Wilson spectroscopic data. In particular, our new measurements of the stellar rotational period $P_{rot} \approx 12.5$ d and of the main principal magnetic cycle of ≈ 12 a allow us to locate this star in the early main sequence phase of its evolution during which the chromospheric activity is dominated by the superposition of several cycles before the transition to the phase of the magnetic-braking shutdown with the subsequent decrease of the magnetic activity.

Keywords: stars: oscillations, stars: interiors, stars: individual (GJ 504), stars: solar-type

1. INTRODUCTION

Over the last decade, thanks to the successful photometric space missions, CoRoT (Convection, Rotation, and Transits Baglin et al. 2006) and Kepler/K2 (Borucki et al. 2010) mainly conceived for exoplanets, but extremely suitable for detection of stellar pulsations, asteroseismology has produced an extraordinary revolution in astrophysics (e.g. Beck et al. 2012; Bedding et al. 2011;

41 [Silva Aguirre et al. 2015](#); [Stello et al. 2016](#)). This unveiled a wealth of results on the physical properties of stars over a large part
42 of the H-R diagram and mostly for solar-like stars, which exhibit pulsations excited by near-surface turbulent convection, as it
43 happens in the Sun.

44 The extreme photometric precision made these missions spectacularly successful also in their primary goal: the detection
45 and characterization of extra-solar planetary systems by using the transit technique ([Borucki et al. 2013](#)). Thus, in recent years
46 a flood of very high-quality data has been collected and the search for new worlds is in progress and we are living exciting
47 times in this respect. Despite the incredible effort in refining observational and post-processing techniques, our interpretation
48 and comprehension of planetary systems architecture, formation and evolution mechanisms heavily relies on the accuracy of the
49 inferred characteristics of the host stars and the effects on their planets ([Van Eylen et al. 2014](#); [Borucki et al. 2013](#); [Huber et al.
2013](#); [Chaplin et al. 2013](#)). This often represents a significant challenge, especially for isolated field stars ([Soderblom et al. 2014](#)).

51 The most recently launched NASA space mission Transiting Exoplanet Survey Satellite, TESS ([Ricker et al. 2014](#)), is poised to
52 continue the synergy between asteroseismology and exoplanet science, enlarging the held of asteroseismic inference to full-sky.
53 Indeed, with the original high-cadence mode of 120-s (Nyquist frequency of $4166 \mu\text{Hz}$) used during the first two years of its main
54 mission and the newer fast cadence of 20-s that started during the extended mission, TESS should be able to detect oscillation in
55 many main-sequence solar-like stars in spite of their low intrinsic amplitudes of parts-per million ([García & Ballot 2019](#)).

56 According to the TESS Asteroseismic Target List ([Schofield et al. 2019](#); [Campante et al. 2016](#)), thousands of main-sequence
57 and subgiant solar-like stars should show detectable modes. So far, signatures of such oscillations have been detected only in a
58 handful of solar-like stars (e.g., [Gandolfi et al. 2018](#); [Huber et al. 2019](#); [Chontos et al. 2020](#); [Metcalf et al. 2020](#); [Addison et al.
2021](#); [Metcalf et al. 2021](#)). Recently, [Huber et al. \(2021\)](#) compared the power spectra of three stars observed by TESS with both
60 cadences of 2-min and 20-s. While the modes were barely visible with the 2-min cadence, the faster cadence drastically increased
61 the signal-to-noise ratio allowing the characterization of the individual modes. Part of this improvement could be explained by
62 the difference of the cosmic-ray rejection applied to both cadences. However, the difficulties to detect the oscillation modes could
63 also be due to the properties of the stars.

64 The non-detection of modes has been investigated also in many stars observed by the *Kepler* mission. For solar-like stars, the
65 usual explanation is the surface magnetic activity of the star (e.g., [Chaplin et al. 2011a](#)) as it is known that a high level of magnetic
66 activity can reduce the amplitude of the modes ([García et al. 2010](#); [Kiefer et al. 2017](#); [Santos et al. 2018](#)) Nevertheless this is not
67 the only culprit as shown in [Mathur et al. \(2019a\)](#). Indeed metallicity or binarity can also have an impact on the amplitude of the
68 modes ([Gaulme et al. 2020](#)).

69 Here, we present the result of the analysis of the solar-type star GJ 504 (spectral type G0), which was observed by the TESS
70 mission for 27 days during sector 23 from March 18, 2020 to April 16, 2020 using 2 minutes cadence mode. Furthermore,
71 spectroscopic observations from the Mount Wilson Observatory are also studied to better characterize the surface magnetic
72 activity of the star.

73 GJ 504 is considered a very interesting case study, claimed to host a sub-stellar companion whose nature is strongly debated.
74 Nevertheless, asteroseismology might provide the only powerful mean to dissolve any doubts about the evolutionary state of this
75 target and hence on the identity of the secondary object. In fact, the detection of typical signatures of solar-like oscillations in the
76 power spectrum would define with good accuracy the age and all the physical parameters of this low-mass star (e.g., [Di Mauro
et al. 2004](#); [Di Mauro 2016](#)). There are many methods to estimate the age of a single star ([Soderblom et al. 2014](#)): empirical
78 indicators such as stellar activity and gyrochronology which link rotation to age (e.g., [Skumanich 1972](#); [Barnes 2007](#); [Mamajek
& Hillenbrand 2008](#)); photospheric lithium abundance (e.g. [Li et al. 2012](#)); comparison of stellar model isochrones with observed
80 classical parameters (e.g. [Pont & Eyer 2004](#)). However, the accuracy that can currently be reached by using all these methods
81 is not satisfactory, not only because of the large errors in the estimates, but also because better precision and accuracy can be
82 reached only by using seismic diagnostics (see, e.g., [Metcalf et al. 2010](#); [Lebreton et al. 2014](#); [Lebreton & Goupil 2014](#)).

83 This paper is organized in the following sections: Section 2 introduces the reader to the target presenting the spectroscopic
84 fundamental parameters and the theoretical predictions deduced by means of stellar evolutionary models and asteroseismic scaling
85 laws; Section 3 presents the observations and the data calibration used in this work; in Section 4, we study the surface rotation
86 and magnetic activity of the this star; in Section 5, we describe the search for solar-like oscillations; Section 6 discusses the
87 reasons for the non detection of solar-like oscillations and presents the attempt to characterize the structure of this star; Section 7
88 shows the conclusions.

89 2. THE SOLAR-LIKE STAR GJ 504

90 2.1. An intriguing case

During the last 25 years, several dedicated space missions, together with great developments in observational techniques, have allowed huge progresses in the search for new worlds outside the solar system. In particular, besides statistics, several hundreds of bright stars have been monitored and multi-wavelengths data collected in order to understand and characterize the formation and the evolution of the already discovered planetary systems.

A controversial case still debated today is represented by the solar-type star GJ 504 (HD 115383, TIC 397587084), a G0-type star with $T_{\text{eff}} \approx 6200 \text{ K}$, which appears to be a little more massive than the Sun (Kuzuhara et al. 2013; D’Orazi et al. 2017), with a rotational period $P_{\text{rot}} = 3.329$ days, average of the values reported by Messina et al. (2003) and Donahue et al. (1996). In 2013, by exploiting high-contrast near-IR and L’-band observations, Kuzuhara et al. (2013) identified a Jovian planet orbiting this star. Employing the gyrochronology technique, based on the stellar chromospheric activity indexes (as given by the Ca II H and K emission lines) and on X-ray observations (the star is included in the ROSAT catalogue), Kuzuhara et al. (2013) estimated the age of GJ 504 to be $Age = 160_{-60}^{+350}$ Myr. Under this assumption, the comparison of observational data with theoretical models implies that the mass of the sub-stellar companion (named GJ 504b) should be $M_{\text{P}} = 4_{-1.0}^{+4.5} M_{\text{Jup}}$. According to Kuzuhara et al. (2013), the measured characteristics make GJ 504b a very interesting object because it represents the first example of giant planet on a wide orbit around a solar-type star. Moreover, the planet appears to be significantly cool ($T_{\text{eq}} = 510_{-20}^{+30} \text{ K}$), with an almost cloud-free atmosphere due to its blue color ($J - H = -0.23$) and, as reported by Janson et al. (2013), represents the first known extrasolar planet with methane-dominated atmosphere (T-type).

However, few years later the young age of GJ 504 has been disproved by Fuhrmann & Chini (2015), thanks to evidences arising from high-resolution and high-quality spectra. In fact, the authors derived a stellar gravity of $\log g = 4.23$ dex (from the Hipparcos parallax and adopting spectroscopic temperature), which results to be not compatible with a stellar age of few hundreds Myr. This gravity estimate is also in agreement with the value of $\log g = 4.17$ dex previously determined in Fuhrmann (2004), based on the spectral fitting of Mg Ib lines and several independent spectroscopic studies and position of the star in the color-magnitude diagram (see, e.g., da Silva et al. 2012). This picture implies that GJ 504 should be a star with approximately the solar age and, as a consequence, the companion has to be identified as a brown dwarf ($M_{\text{P}} \sim 25M_{\text{Jup}}$) rather than a giant planet. In order to explain the relatively high stellar rotation velocity and chromospheric activity level of the host star, and reconcile isochronal ages with direct indicators, Fuhrmann & Chini (2015) invoked a merging event. GJ 504 might have engulfed a sub-stellar companion that is responsible for speeding up the rotational velocities and accounts for the enhanced activity levels (Oetjens et al. 2020).

D’Orazi et al. (2017), reassessing the properties of GJ 504, have found that the surface gravity of the star implies an evolutionary stage obtained by the isochrones comparison which suggests an age range between 1.8-3.5 Gyr (most probable age ≈ 2.5 Gyr). To reconcile all the age indicators and to explain the high level of activity, also these authors suggest a merging scenario (more recent than 200 Myr) with a very close hot Jupiter companion.

The system has been recently revisited by Bonnefoy et al. (2018) by using interferometric, radial-velocity, and high-contrast imaging observations. They found an interferometric radius of $R = (1.35 \pm 0.04)R_{\odot}$ for GJ 504, which is compatible with two isochronal age ranges (21 ± 2) Myr and (4.0 ± 1.8) Gyr. According to this work, the mass of GJ 504b is expected to be $M_{\text{P}} = 1.3_{-0.3}^{+0.6} M_{\text{Jup}}$ for the young age case and $M_{\text{P}} = 23_{-9}^{+10} M_{\text{Jup}}$ for the old one.

Therefore, the evolutionary stage and the age of GJ 504 is still an open problem with no clear solution to date. This uncertainty closely concerns the mass estimation of the star’s companion, which could be a Jovian planet or a brown-dwarf. In addition, Skemer et al. (2016), through a photometric study, suggested for GJ 504b a higher metallicity ($[M/H]_{\text{p}} \approx +0.6$) with respect to the host star ($[Fe/H]_{\star} \approx +0.1 - 0.3$), adding to this system another element of interest.

For all the above mentioned reasons the GJ 504 system constitutes an intriguing case which, deserves to be carefully studied, with the aim of shedding light on the age of the star and, accordingly, on the nature of the sub-stellar companion.

2.2. Fundamental parameters

In order to properly characterize this star we performed an analysis of the broadband Spectral Energy Distribution (SED) together with the *Gaia* EDR3 (*Gaia* Collaboration 2018) parallax measurement following the procedures described in Stassun & Torres (2016), Stassun et al. (2017), and Stassun et al. (2018). The input parameters and the obtained results are summarized in Table 1. We employed the *UBV* magnitudes from Mermilliod (2006), the $B_T V_T$ magnitudes from *Tycho-2*, the Strömgren *uvby* magnitudes from Paunzen (2015), the *JHK_S* magnitudes from 2MASS, the W1–W4 magnitudes from *WISE*, and the FUV magnitude from *GALEX*. The available photometry, all together, spans the full stellar SED over the wavelength range 0.2–22 μm (Fig. 1).

We performed a fit using Kurucz stellar atmosphere models, with the T_{eff} , $\log g$, $[Fe/H]$, and $v \sin i$ taken from the spectroscopic analysis of D’Orazi et al. (2017). The remaining parameter is the extinction (A_V), which we fixed to be zero due to the star’s proximity. The resulting fit is shown in Fig. 1, obtained with a reduced $\chi^2 = 1.9$. Integrating the model SED gives the bolometric

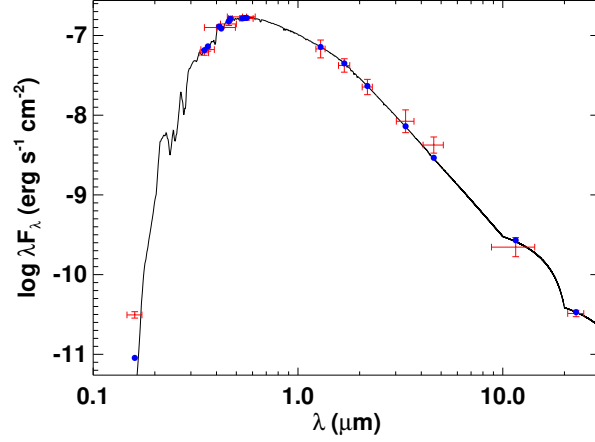


Figure 1. Spectral energy distribution. Red symbols represent the observed photometric measurements, where the horizontal bars represent the effective width of the pass-band. Blue symbols are the model fluxes from the best-fit Kurucz atmosphere model (black).

Table 1. The fundamental parameters of GJ 504 (TIC 397587084).

Basic Properties	
TESS Magnitude	4.6552 ± 0.0073^a
π (mas)	57.0186 ± 0.2524^b
Spectroscopic parameters ^c	
T_{eff} (K)	6205 ± 20
[Fe/H] (dex)	0.22 ± 0.04
$v \sin i$ (km s ⁻¹)	2.8 ± 1.6
log g (dex)	4.29 ± 0.07
SED results	
F_{bol} (erg s ⁻¹ cm ⁻²)	$(2.10 \pm 0.02) \cdot 10^{-8}$
L_{SED}/L_{\odot}	2.01 ± 0.03
M_{SED}/M_{\odot}	1.07 ± 0.17
R_{SED}/R_{\odot}	1.227 ± 0.012
P_{SED} (d)	2.4 ± 1.3
Age_{SED} (Gyr)	0.2 ± 0.2
SBCR results	
$\theta_L D$ (mas)	0.622 ± 0.122
$R_{\text{SBCR}}/R_{\odot}$	1.176 ± 0.192

Notes:

^a Adopted from the TESS Input Catalog (Stassun et al. 2019).

^b Gaia measurement (see Gaia Collaboration 2018)

^c Determined by spectroscopic observations (see D’Orazi et al. 2017)

143 flux at Earth of $F_{\text{bol}} = (2.096 \pm 0.024) \cdot 10^{-7}$ erg s⁻¹ cm⁻². Taking the F_{bol} and T_{eff} together with the *Gaia* parallax, with no
 144 adjustment for systematic parallax offset (see, e.g., Stassun & Torres 2021), gives the stellar radius as $R_{\text{SED}} = (1.227 \pm 0.012)R_{\odot}$.
 145 The F_{bol} and parallax also yield directly the bolometric luminosity, $L_{\text{SED}} = (2.01 \pm 0.03)L_{\odot}$.

The empirical stellar radius determined above affords an opportunity to estimate the stellar mass empirically as well, via the spectroscopically determined surface gravity, obtaining $M_{\text{SED}} = (1.07 \pm 0.17) M_{\odot}$. This value is consistent with that estimated via the eclipsing-binary based relations of [Torres et al. \(2010\)](#).

Using the activity-age relations of [Mamajek & Hillenbrand \(2008\)](#), we obtained from R'_{HK} and the star's $B - V$ color, an age of $\text{Age}_{\star} = (0.2 \pm 0.2)$ Gyr and a rotational period for the star of $P_{\text{SED}} = (2.4 \pm 1.3)$ days which is consistent with previous findings of 3.3 days ([Donahue et al. 1996](#); [Messina et al. 2003](#); [Wright et al. 2011](#)).

In order to get another independent measurement of the stellar radius, it is also possible to employ the approach based on the Surface-Brightness Colour relationships (SBCR), which allows to easily estimate the limb-darkened angular diameter of the star. The latter combined with the distance of the star provides the linear stellar radius.

Considering the SBCR from [Salsi et al. \(2021\)](#) obtained for late-type dwarf stars (their Table 4), $m_G = 5.0398 \pm 0.0029$ mag ([Gaia Collaboration 2020](#)), $m_K = 4.033 \pm 0.238$ mag ([Cutri et al. 2003](#)), and $A_V = A_g = 0.0$ mag derived from [Stilism](#) tool ([Lallement et al. 2014](#); [Capitaino et al. 2017](#)), as well as $A_K = 0.089A_V$ ([Nishiyama et al. 2009](#)), we find $\theta_L D = 0.622 \pm 0.014 \pm 0.008 \pm 0.100$ mas. The uncertainties correspond respectively to the RMS of the SBCR, the uncertainty on the coefficients of the SBCR and the uncertainty on the G and Ks photometries. Using Gaia DR2 parallax, i.e. $\pi = 56.8577 \pm 0.1224$ mas ([Gaia Collaboration 2020](#)), we obtain $R_{\text{SBCR}} = (1.176 \pm 0.027 \pm 0.015 \pm 0.19 \pm 0.003)R_{\odot} = (1.176 \pm 0.192)R_{\odot}$, where the error 0.003 is rising from the uncertainty on the Gaia parallax. This value agrees within the uncertainty with the SED estimate found above.

2.3. The seismic properties and the asteroseismic prediction by scaling laws

The properties of a solar-like pulsating star can be described by adopting the asymptotic development by [Tassoul \(1980\)](#), which predicts that the oscillations excited in main-sequence stars are acoustic modes (p modes) with frequencies $\nu_{n,l}$ characterized by radial order n and harmonic degree l , which for $l \leq n$ should satisfy the following approximation:

$$\nu_{n,l} \sim \Delta\nu \left(n + \frac{l}{2} + \epsilon \right), \quad (1)$$

where ϵ is a function of frequency and depends on the properties of the surface layers and $\Delta\nu$, known as the large frequency separation, is the inverse of the sound travel time across the stellar diameter:

$$\Delta\nu = \left(2 \int_0^R \frac{dr}{c} \right)^{-1}, \quad (2)$$

where c is the local speed of sound at radius r and R is the photospheric stellar radius. Hence, according to the theory, the solar-like oscillations spectrum of GJ 504 should show a series of equally spaced peaks separated by $\Delta\nu$ between p modes of same degree l and adjacent n :

$$\Delta\nu \approx \nu_{n+1,l} - \nu_{n,l} \equiv \Delta\nu_l. \quad (3)$$

In addition, the power spectra of this target should show another series of peaks, whose separation $\delta\nu_l$ is known as the small separation:

$$\delta\nu_l \equiv \nu_{n,l} - \nu_{n-1,l+2} \quad (4)$$

which is sensitive to the chemical composition gradient in the central regions of the star and hence to its evolutionary state. Thus, the determination of the large and small frequency separations from the observed oscillation spectrum can directly provide asteroseismic inferences on the mass and the age of GJ 504 ([Christensen-Dalsgaard 1988](#)).

The observed oscillation power spectrum of the solar-like stars is characterized by a typical Gaussian like envelope and the frequency of maximum oscillation power is usually indicated by ν_{max} . As conjuctered by [Brown et al. \(1991\)](#), the frequency ν_{max} can be related to the acoustic cutoff frequency ν_{ac} , which defines the upper boundary of the p mode resonant cavities:

$$\nu_{\text{max}} \propto \nu_{ac} \propto g T_{\text{eff}}^{-1/2}, \quad (5)$$

Thus, according to Eq. 5, the frequency ν_{max} carries information on the physical conditions in the near-surface layers of the star. Thus, as it has been well demonstrated both theoretically ([Chaplin et al. 2008](#); [Belkacem et al. 2011](#)) than observationally ([Bedding & Kjeldsen 2003](#); [Stello et al. 2008](#); [Bedding 2014](#)), as a solar-type star evolves, its oscillation spectrum moves towards lower frequencies due to the decrease of the surface gravity.

In order to extract a rough estimate of the asteroseismic parameters of the star to be adopted as guess values for the oscillation analysis, it is possible to assume well proved scaling-laws as those provided by (see, e.g., [Brown et al. 1991](#); [Kjeldsen & Bedding](#)

Table 2. Predictions for the frequency of maximum oscillation computed assuming spectroscopic data obtained by different authors .

T_{eff}	$\log g$	ν_{max}	Reference
(K)	(cm/s ²)	(μ Hz)	
6205 \pm 20	4.29 \pm 0.07	2096 \pm 338	D’Orazi et al. (2017)
5978 \pm 60	4.23 \pm 0.10	1860 \pm 428	Fuhrmann & Chini (2015)
6130 \pm 48	4.33 \pm 0.10	2312 \pm 533	Maldonado et al. (2015)
6185 \pm 51	4.30 \pm 0.07	2148 \pm 346	Battistini & Bensby (2015)
5995 \pm 41	4.24 \pm 0.02	1900 \pm 88	Ramírez et al. (2013)
6012 \pm 100	4.30 \pm 0.20	2179 \pm 100	Mishenina et al. (2013)
6234 \pm 25	4.60 \pm 0.02	4269 \pm 197	Valenti & Fischer (2005)

195), and by Huber et al. (2011). These relations, which have been typically calibrated on large samples of main-sequence stars, offer the possibility to predict the range of frequencies where the excess of power for a given solar-like star will manifest. By assuming the relations by Kjeldsen & Bedding (1995) and Kjeldsen et al. (2008), we calculated the value of the expected maximum amplitude of oscillation A_{max} and the frequency at the maximum amplitude ν_{max} , using the observed surface gravity g and the effective temperature T_{eff} of the star. By using scaling relations and corrections by Campante et al. (2016) we obtained a value for the expected maximum amplitude in the range $A_{\text{max}} = (2.51 - 2.95)$ ppm depending on which input spectroscopic parameters are assumed.

Table 2 shows the results for the expected ν_{max} computed assuming spectroscopic measurements published by different authors. Except for the ν_{max} from the stellar parameter of Valenti & Fischer (2005), who reported a high surface gravity, all the expected values for the frequency of maximum oscillation lie in the range (1800-2300) μ Hz. Thus, if there is an excess of power due to oscillations in the GJ 504 spectrum, we expect to find it in this range of frequencies.

2.4. Theoretical prediction by evolutionary models

Given the observed fundamental parameters collected in Table 1, it is also possible to face the theoretical challenge to infer the structural properties of GJ 504 and predict its detailed oscillation spectrum by constructing stellar evolutionary models which satisfy the observational constraints.

We produced theoretical structure models for the star by using the ASTEC evolutionary code (Christensen-Dalsgaard 2008a) by varying the mass and the composition in order to match the atmospheric parameters available. The resulting evolutionary tracks characterized by fixed mass M and initial chemical composition have been calculated with the OPAL 2005 equation of state (Rogers & Nayfonov 2002), OPAL opacities (Iglesias & Rogers 1996), and the NACRE nuclear reaction rates (Angulo et al. 1999). Convection was treated according to the mixing-length formalism (MLT) (Böhm-Vitense 1958) and defined through the parameter $\alpha = \ell/H_p$, where H_p is the pressure scale height and α is assumed to be 1.8. The initial heavy-element mass fraction Z in respect to the abundance of the hydrogen X has been calculated from the iron abundance given in Table 1 using the relation $[\text{Fe}/\text{H}] = \log(Z/X)_s - \log(Z/X)_\odot$, where $(Z/X)_s$ is the value at the stellar surface and the solar value was taken to be $(Z/X)_\odot = 0.0245$ (Grevesse & Noels 1993).

Fig. 2 shows a series of evolutionary tracks obtained for different masses and fixed initial composition, plotted in two H-R diagrams, representing respectively the effective temperature-gravity plane and the effective temperature-luminosity plane. The present evolutionary models do not include additional effects such as overshooting, settling of heavy elements and rotation.

The location of the star in the H-R diagram identifies GJ 504 as being at the beginning of the main sequence phase. In fact, only a small percentage of the hydrogen fuel, indicated by X_c in Table 3, has been already converted into helium. The uncertainty in the observed value of Z_s introduces an uncertainty in the determination of the stellar mass whose value, considering only the observed spectroscopic parameters, seems to be limited to the range $M = (1.28 \pm 0.07)M_\odot$ hence slightly more massive than the Sun, in agreement with the value predicted by SED analysis (see Section 2.2). The stellar radius appears $R = (1.38 \pm 0.20)R_\odot$,

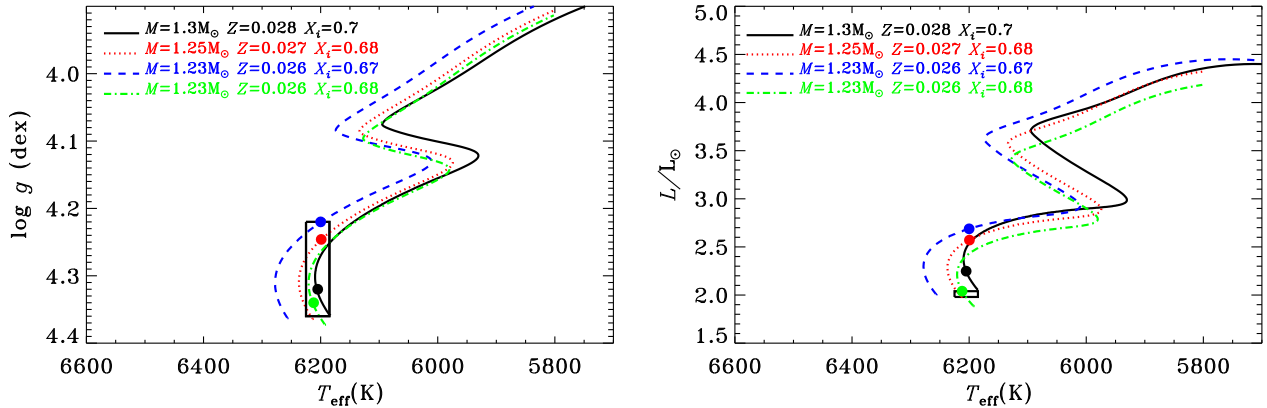


Figure 2. Evolutionary tracks plotted in two plans of the H-R diagram calculated for different values of the mass and the metallicity, while all the other parameters are fixed. The initial hydrogen abundance is X_i and the mixing-length coefficient is $\alpha = 1.8$. The rectangle defines the one-sigma error box for the observed gravity and effective temperature. Coloured dots indicate the position of the four structure models (see Table 3) which best reproduce the observations of GJ 504.

a value which is in good agreement within the errors, not only with the estimates found in Sec. 2.2 by the SED and the SBCR methods, but also with the most accurate interferometric radius measured by Bonnefoy et al. (2018).

The age of this star, as obtained from the evolutionary models, can be estimated in the range 0.0 – 2.6 Gyr, hence younger than the Sun, so that the convective envelope should appear still quite shallow with a depth not larger than $D_{cz} \approx 0.16R$. Thus, we confirm that GJ 504 is a very young star as we found in Sec. 2.2 by SED calculations and in agreement, within the quoted uncertainties, with the values by D’Orazi et al. (2017) and by Kuzuhara et al. (2013), while our stellar structure models do not show a star of solar age as supposed by Fuhrmann & Chini (2015); Bonnefoy et al. (2018).

In order to predict the observed pulsational scenario of GJ 504, we used the ADIPLS package (Christensen-Dalsgaard 2008b) to compute theoretical adiabatic oscillation frequencies for all the structure models satisfying the spectroscopic constraints. The theoretical result show that the oscillation modes expected to be visible in this star should be $l = 0, 1, 2, 3$ pure acoustic modes with frequencies in the range approximately between $(1500 - 3500) \mu\text{Hz}$ while the theoretical large separation calculated by linear fit over the asymptotic relation for the radial mode frequencies appear to be $\Delta\nu = (98 \pm 13) \mu\text{Hz}$.

Among all the possible computed structure models, we selected four models chosen in order to best-fit the observed effective temperature, the metallicity and the gravity (Table 1) and with location in the HR diagram shown by coloured dots (see Fig. 2).

In Table 3 we give a comprehensive set of physical properties for the four different models of GJ 504. In particular Model 1 has been chosen in order to match within 1σ also the luminosity obtained by the SED technique (see Table 1).

We expect to be able to distinguish among the different models of this target by measuring at least the large separation in the observed oscillation spectrum.

3. OBSERVATIONS AND DATA PREPARATION

GJ 504 was observed by TESS during 27 consecutive days of sector 23 from March 18, 2020 to April 16, 2020. In order to perform the seismic analysis and due to the high-level of noise of the TESS 120-s cadence data for this star, we adopted four different strategies to obtain seismically optimized light curves. In such way we ensure that the obtained results are independent of the methodology applied.

The first methodology exploits TESS Science Processing Operations Center (SPOC, Jenkins et al. 2016) pipeline light curve, with a cadence of 120 s, available on the MAST archive¹. This raw light curve shows strong modulations at low frequency that is filtered out by applying a smoothing removal process iterated three times. The resultant residuals are subsequently $3 - \sigma$ -clipped to eliminate any outliers as depicted in panel (a) of Fig. 3.

The second methodology started with the TESS SPOC 120 s cadence target pixel files. We then extracted a time series for each pixel, rejecting cadences with nonzero quality flags (see for details the TESS Science Data Products Document²), and constructed

¹ <https://archive.stsci.edu/hlsp/tess-spoc>

² <https://archive.stsci.edu/missions/tess/doc/EXP-TESS-ARC-ICD-TM-0014.pdf>

Table 3. Main parameters for four best-fit structure models of GJ 504.

	Model 1	Model 2	Model 3	Model 4
M/M_{\odot}	1.23	1.23	1.25	1.30
Age (Gyr)	0.66	2.46	2.19	0.74
T_{eff} (K)	6212	6200	6200	6205
$\log g$ (dex)	4.34	4.22	4.25	4.32
R/R_{\odot}	1.23	1.42	1.38	1.30
L/L_{\odot}	2.04	2.69	2.57	2.25
Z_s	0.026	0.026	0.027	0.028
X_s	0.68	0.67	0.68	0.7
X_c	0.58	0.29	0.35	0.59
[Fe/H]	0.19	0.20	0.21	0.21
r_{cz}/R	0.840	0.837	0.846	0.846
α_{MLT}	1.8	1.8	1.8	1.8
$\Delta\nu$ (μHz)	109.6	87.8	90.9	104.5

NOTE— M/M_{\odot} is the mass of the star, T_{eff} is the effective temperature, $\log g$ is the surface gravity, R/R_{\odot} is the surface radius, L/L_{\odot} is the luminosity, Z_s is the surface heavy-element abundance, X_s is the surface hydrogen abundance, X_c is the hydrogen abundance in the core, [Fe/H] is the iron abundance, r_{cz} is the location of the base of the convective region, α_{MLT} is the mixing-length parameter and $\Delta\nu$ is the large separation obtained from the theoretical pulsational frequencies.

251 an aperture mask using the procedure described in (Buzasi et al. 2016) and (Nielsen et al. 2020). Essentially this process produces
 252 a time series with the minimum sum of first differences between successive points. We then adopted sigma-clipping at the 4σ level
 253 combined with simple gap filling through the use of a piecewise cubic hermite interpolating polynomial (PCHIP; as implemented
 254 in Scipy (Jones et al. 2001)). The result is shown in panel (b) of Fig. 3.

255 The third approach is based on a filtering of the SPOC lightcurve using two successive Gaussian filters of width 0.25 and 0.125
 256 days. This was done in order to remove long periodicities and to reduce the noise level. The lightcurve presents a large gap that
 257 could degrade the quality of the spectrum (window effect). The gap was removed before filtering the lightcurve and the first time
 258 stamp was set to zero. The result is shown in panel (c) of Fig. 3.

259 Finally, the last method started from the target pixel file to create a larger aperture. In general, light curves obtained from big
 260 apertures are more stable to small instrumental perturbations such as the loss of pointing of the satellite or to the movement of the
 261 star during the observations. To build this larger aperture, contiguous pixels starting from the center of the target are selected. A
 262 new pixel is selected only if the integrated flux of the pixel has a negative gradient compared to the previous one (decreasing the
 263 flux from the center to avoid any polluting star) and with an average flux greater than a given threshold that has been established
 264 to 100 e-/s. Once this is done, an extra pixel at the top and the bottom of the aperture is added to the 4 central rows, which contain
 265 several saturated pixels. By selecting these extra pixels, the resulting light curve has smaller dispersion around the mean between
 266 the days 1933.5 and 1936. The final aperture is shown in Fig. 4. It is important to notice that no significant changes were found
 267 by adding more pixels to the central rows or by slightly changing the limit threshold of 100 e-/s.

268 To increase the duty cycle, instead of removing all points with a flag different to zero, we applied two different selections of
 269 the NASA quality flags. We either kept all the points except the ones with a flag between 2 and 32 (Dark blue curve in panel (d)
 270 of Fig. 3) or between 2 and 512 (magenta curve in panel (d)) of the same figure). We then calibrated the two resulting lightcurves
 271 following (García et al. 2011), removing outliers, correcting jumps, and drifts. To convert the flux in parts per million (ppm) and
 272 remove the low frequency contribution we used a triangular smooth with a window of half a day. Except for the big gaps in the
 273 middle of the run, all the rest were interpolated using inpainting techniques with a multi-scale discrete cosine transform (García

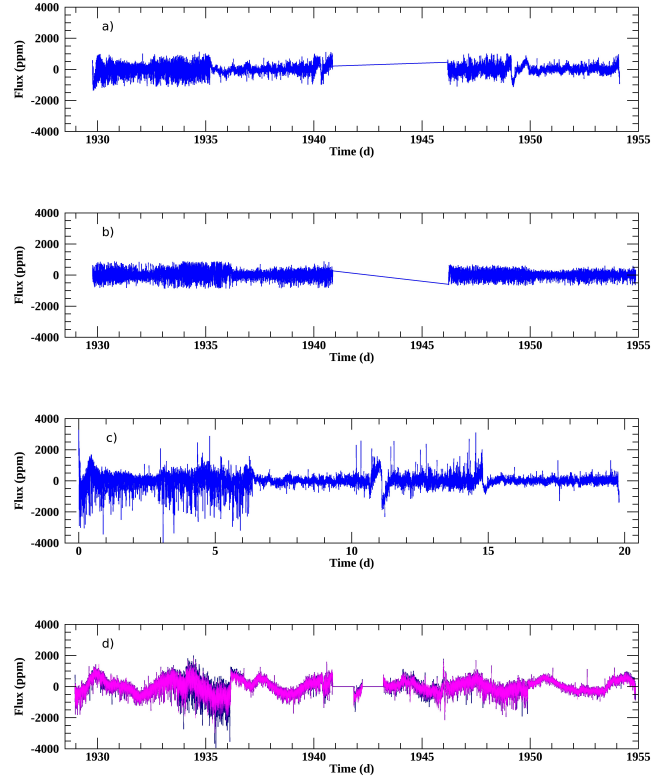


Figure 3. Seismically optimized lightcurves used in this work as explained in Section 3.

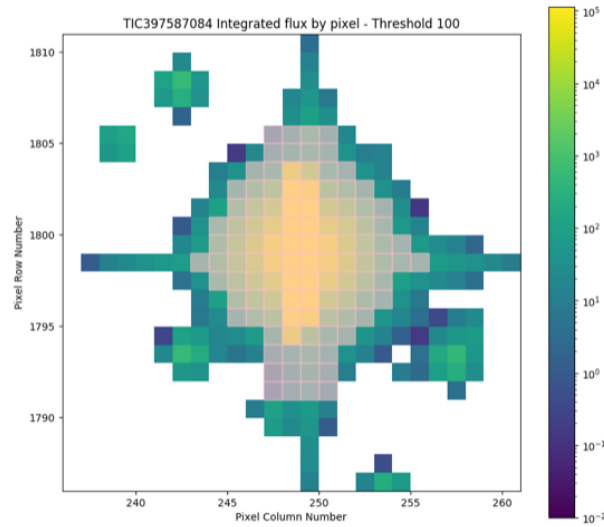


Figure 4. Enlarged mask used in the fourth calibration method described in Sect. 3. The selected pixels are depicted in gray.

274 et al. 2014a; Pires et al. 2015). These two lightcurves are longer and with some more data in the middle of the run than the other
 275 three presented before.

276 In order to do the seismic analysis, the Power Spectral Density (PSD) is computed. As shown in Fig. 5, the PSD is dominated
 277 by flat noise above $\sim 200 \mu\text{Hz}$ and a low-frequency slope below $\sim 60 \mu\text{Hz}$. Hence, the background can be characterized by two
 278 Harvey components (Harvey 1985) and a flat noise level. As expected, the high-frequency Harvey profile (related to convective

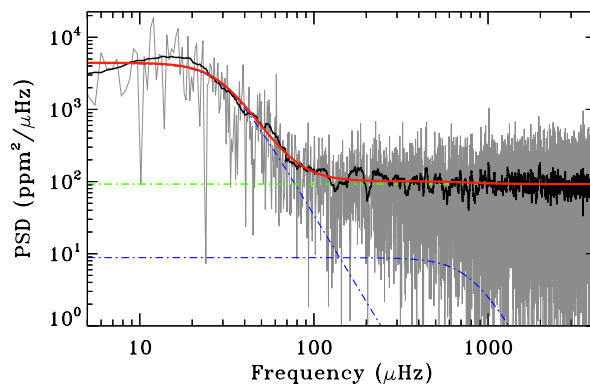


Figure 5. Power spectral density (light gray) with a smoothing overlaid (black curve) of the first seismically optimized lightcurve (shown in panel a) of Fig. 3). The background fit is composed of two Harvey-like profiles (blue curves) and a flat noise level (green curve). The sum of the three components is indicated by the thick red line. No evidence of a Gaussian power excess is found.

noise) has an amplitude of around an order of magnitude smaller than the flat noise component. The low-frequency Harvey profile, with a knee at around $20 \mu\text{Hz}$, is probably related to magnetism and not convection.

GJ 504 is indeed a magnetically active star that was part of a large observational campaign, the HK Project, conducted at the Mount Wilson Observatory (MWO) from 1966 to 1995 with the aim to search for stellar analogs to the solar cycle by studying stellar chromospheric activity and variability (Wilson 1968, 1978). These measurements, available from the National Solar Observatory (NSO) website³, are expressed in term of the dimensionless S-index, defined as the ratio of emission in the Ca II H & K line cores to that in two nearby continuum reference bandpasses (for further details see, e.g., Vaughan et al. 1978; Egeland et al. 2017). For this star, within the MWO dataset, about 1342 single measurements are provided in the time interval 1966-1995, allowing us to study its magnetic activity over a time period of nearly 30 years.

4. ROTATION AND MAGNETIC ACTIVITY ANALYSIS

4.1. Rotation

To determine the surface rotation period of GJ 504, a similar methodology as the one applied to the two last lightcurves described in the previous section is employed but this time smoothing the light curve using a triangular filter (double boxcar function). The width of each boxcar is a fifth of the total length. The obtained rotation period, P_{rot} , is independent of the flags removed in the lightcurve because we are interested on the long periods and thus the extra removed peaks with a bad flag do not affect the calculation. To look for P_{rot} , a methodology combining 3 different techniques is used following, e.g., Santos et al. (2019, 2021). The first method performs a time-frequency analysis using a Morlet wavelet (Torrence & Compo 1998). The second utilizes an auto-correlation function (e.g. Garca et al. 2014b; McQuillan et al. 2014). The third method combines the first two in order to compute the Composite Spectrum (e.g. Ceillier et al. 2016). Hence, a modulation with a periodicity of (3.4 ± 0.25) days is found in the light curve (see Fig. 6).

We also examined the Mount Wilson data to search for a potential rotational periodicity. The data consist of 1342 observations taken between March 1966 and June 1995. Before searching for the presence of a periodicity in the S-index of GJ 504, we visually analyzed the available Mount Wilson data. We noted that 3 measurements taken in 1993, during the same night, are completely outside the mean range of variation (the average MWO S-index for this star is 0.313), with values that are two times larger with respect to all the others. We suspected that such scattered measurements may be the result of an error in the data collection on that night, hence we chose to discard them in the following data analysis of the S-index. We removed the three outliers with S-index values greater than 4σ above the mean, applied a simple linear detrending to the data to remove the lowest-frequency signal, and analyzed the resulting time series using both a DFT and a Lomb-Scargle periodogram. The former results in an estimated rotation period $P_{\text{rot}} = (12.5 \pm 2.8)$ days, while the latter produces (11.8 ± 2.4) days, with uncertainties estimated based on the width of the periodogram peaks. Note that while the Lomb-Scargle peak is significant ($\text{SNR} > 7$) the DFT peak only has a $\text{SNR} \sim 3$ relative to the local background, so we would qualify this period as suggestive but not conclusive.

³ <https://nso.edu/data/historical-data/mount-wilson-observatory-hk-project/>

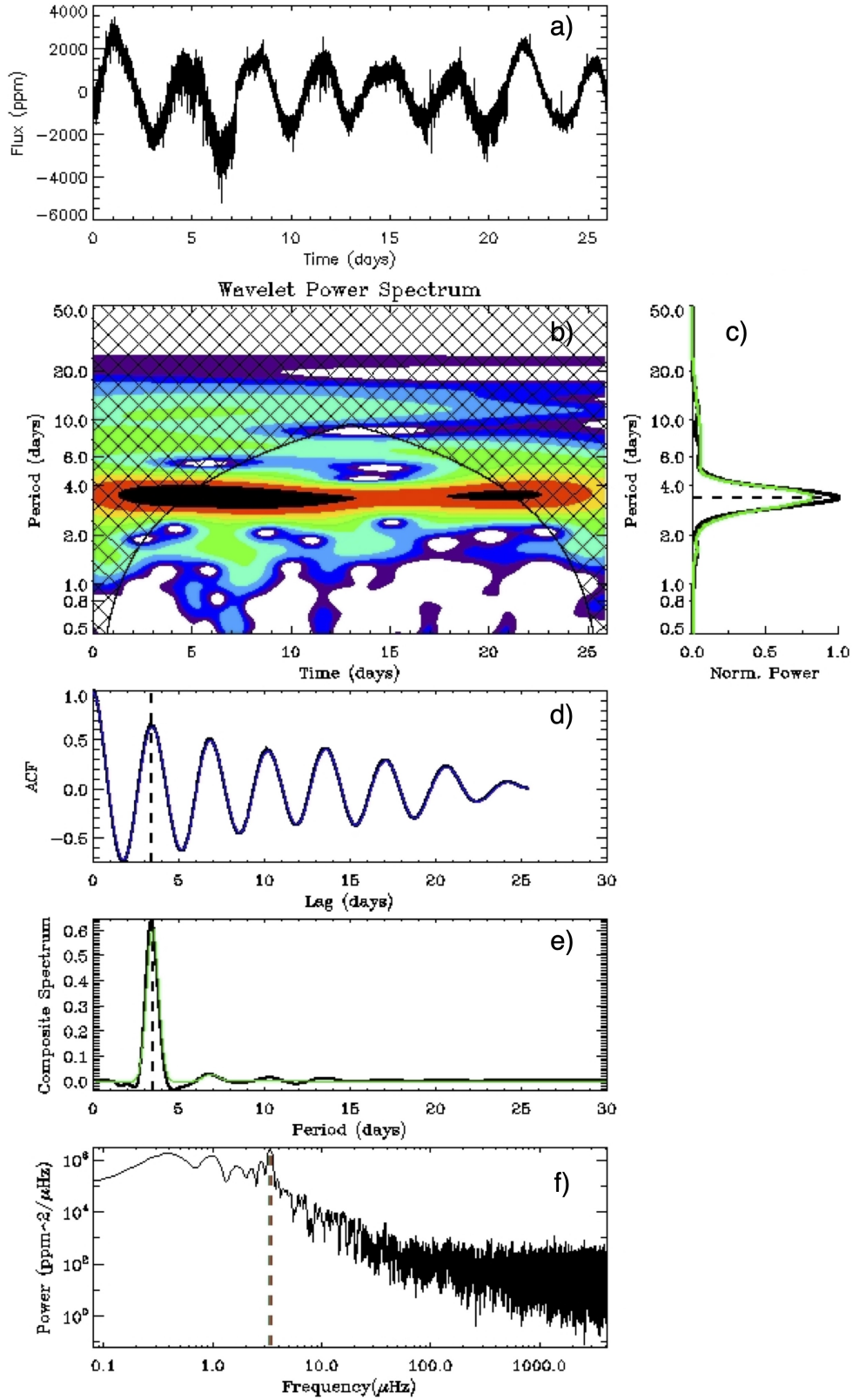


Figure 6. (a) TESS lightcurve for the rotation analysis. (b) Time-period analysis using wavelets. Black corresponds to high power and blue to low power. Black hatched area represents the region that cannot be sampled with the current length of the lightcurve. (c) Projection of the period-time analysis onto the period axis (black) and corresponding fits with multiple Gaussian functions (green). (d) Autocorrelation function. (e) Composite Spectrum (black) and best Gaussian fit (green). (f) PSD in logarithmic scale. The black dotted line indicates the rotation-period estimate.

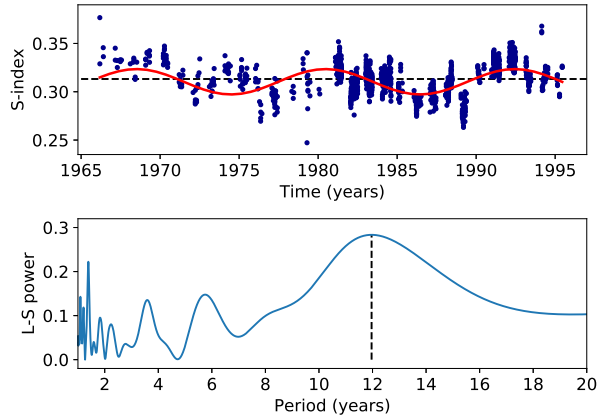


Figure 7. *Top panel:* Mount Wilson S-index measurements for the time interval 1966-1995. The dashed black line indicates the mean S-index. The red line shows the sinusoidal fit to the highest peak as provided by the periodogram in the bottom panel. *Bottom panel:* Lomb-Scargle periodogram of the S-index. The highest peak corresponds to a cycle period of $\approx 12 a$.

310 Given the short length of the TESS lightcurve, it is possible that the periodicity found of ≈ 3.4 days is a harmonic of the
 311 real P_{rot} , and the Mount Wilson period is indeed consistent with that interpretation. Longer high-quality time series would be
 312 necessary to conclude on the actual rotation period of this star.

313 4.2. Magnetic activity and cycles

314 While determining the magnetic activity level and the eventually presence of a periodic variability of a star (i.e., a stellar
 315 cycle), a key role is played by long-term datasets providing measurements of chromospheric proxies. As known from literature,
 316 many stars other than the Sun show a chromospheric variability related to magnetic activity which exhibit periodic variations
 317 (see e.g., Baliunas et al. 1995; Hall 2008). A periodic variability is typically visible also in the photospheric emission, whose
 318 phase difference with the chromospheric one reveals the activity dominant regime of the star, i.e. faculae-dominated (phase) or
 319 spot-dominated (anti-phase) (Radick et al. 1998; Reinhold et al. 2019). Before searching for the presence of a periodicity and to
 320 assess its level of magnetic activity, as in Sec. 4.1, we chose to discard the 3 outliers measurements in the following data analysis
 321 of the S-index.

322 In order to evaluate the magnetic activity level of the star, we firstly computed the average S-index over the whole time interval
 323 (1966-1995) as well as its extreme values. The data are shown in the top panel of Fig. 7. The mean S-index is 0.313, while the
 324 minimum and maximum values are respectively 0.247 and 0.377. If we compare the mean value with the solar one for cycle 23
 325 (0.170), as reported by Egeland et al. (2017), we can infer that the mean MWO S-index of GJ 504 is around 1.8 times that of
 326 the Sun. In addition, the variability in the S-index (~ 0.13), i.e., the difference between the maximum and minimum values, is
 327 greater than that of the Sun during a solar cycle (~ 0.02). We are, therefore, facing a star whose chromospheric activity level is
 328 much higher with respect to that of a reference star like the Sun, pointing towards a probable age smaller than the solar one due
 329 to the fact that chromospheric activity typically decreases as the star evolves (Skumanich 1972; Mamajek & Hillenbrand 2008;
 330 Fabbian et al. 2017; Gondoin 2018).

331 To search for a long-term periodic variation, the observations of the S-index from the Mount Wilson Observatory available for
 332 a large number of stars, constitute a very useful tool. To do that we use an algorithm largely employed in astrophysics, the Lomb-
 333 Scargle periodogram (Lomb 1976; Scargle 1982) which, unlike the more classical Fourier analysis, allows to identify periodicity
 334 in unevenly sampled data, as in the case of the Mount Wilson observations. The computed Lomb-Scargle periodogram of GJ 504
 335 is shown in the bottom panel of Fig. 7. Despite the presence of some peaks at small time scales (1.39, 3.59, and 5.75 a), partially
 336 due to the data sampling, the highest one corresponds to a main periodicity of 11.97 a. The corresponding false alarm probability
 337 (FAP) is $7.97 \cdot 10^{-93}$, indicating that the detected cycle period is statistically significant and unambiguous. This result indicates for
 338 this star the presence of a principal periodic chromospheric variability with a characteristic time quite similar to the Sun Schwabe
 339 11-year cycle, even if it is set to a higher level of activity compared to the latter.

340 In addition to measuring the magnetic activity of GJ 504 with spectroscopic data, we also computed the photometric magnetic
 341 activity index, S_{ph} using TESS data. Following Mathur et al. (2014b,a), it is computed as the standard deviation of subseries of
 342 length $5 \times P_{\text{rot}}$ to ensure that we are measuring the variability due to the magnetic activity. From that temporal $S_{\text{ph}}(t)$, we take the
 343 mean value. Using the rotation period of 3.4 days found in Section 4.1, we obtain $S_{\text{ph}} = (1231 \pm 7.8)$ ppm.

5. SEARCHING FOR SOLAR-LIKE OSCILLATIONS

Based on the spectroscopic parameters of GJ 504, we looked for the solar-like oscillations using the prediction from Sects 2.3 and 2.4. As seen on Figure 5, the modes are not obvious and hence, we applied global seismic methods to look for the global seismic parameters.

In order to confirm the results obtained, the analysis of the power spectrum was independently performed by 4 teams who adopted different methods as described below.

The first method consisted in searching for the presence of oscillations in a region centered around 2000 μHz , as suggested by the former predictions for ν_{max} . For this purpose we adopted the public tool DIAMONDS⁴ (Corsaro & De Ridder 2014) coupled with the Background code extension⁵ for estimating the level of the background signal. The background signal, as described in Corsaro et al. (2017), comprises two Harvey-like profiles accounting for possible granulation-related signal and other variations at low frequency, a flat instrumental noise, and a Gaussian envelope of the solar-like oscillations. In particular we performed a Bayesian model comparison by means of the Bayesian evidence computed by DIAMONDS to select the best competing background model between one including the Gaussian envelope of the solar-like oscillations and one excluding it (see also Müllner et al. 2021). The resulting Bayes' factor suggests that the incorporation of an additional Gaussian profile is not statistically justified, meaning that in the light of the current data-set we could not detect the presence of a power excess due to stellar oscillations in this star. This result is depicted in Fig. 5, where no clear power excess due to stellar oscillations can be observed.

With the second method (applied to the second set of lightcurve), we searched for peaks in the resulting amplitude spectrum, requiring a minimum separation between peaks of 20 μHz , and generated an upper envelope across those peaks using cubic spline interpolation. The peak location of the resulting envelope, which represents ν_{max} was estimated by fitting a Gaussian, and uncertainties in the resulting peak location estimated by a Monte Carlo simulation that allowed the minimum separation to vary between [0, 40] μHz . To estimate the large separation ν_{max} , we performed an autocorrelation of the central 400 μHz of the amplitude spectrum, and used the Monte Carlo process to quantify the uncertainty in that estimate. This process resulted in $\nu_{\text{max}} = 1919 \pm 40 \mu\text{Hz}$ and $\Delta\nu = 85.0 \pm 3.6 \mu\text{Hz}$. However, the peak envelope height is not large enough to claim statistical significance for this result, though it is suggestive and we will use this value for comparison with the theoretical models.

The third pulsation search algorithm is an upgraded version of Benomar et al. (2012) and was applied to the third lightcurve described in Section 3. The first step consists in getting initial guesses for a Bayesian analysis that follows if pulsations are detected conclusively. A first power spectrum F_{noise} of the star is produced by heavily smoothing (box-car smoothing of width $\approx 100 \mu\text{Hz}$) the original power spectrum. This allows to have an approximation of the noise background as pulsations (if any) are damped by the smoothing. A second spectrum F_{modes} is produced using a smoothing coefficient (box-car smoothing of $\approx 0.8 \mu\text{Hz}$) optimised for revealing individual pulsations. The maximum of amplitude of the ratio $F_{\text{modes}}/F_{\text{noise}}$ is then estimated by performing a local 3rd order polynomial fit. The FWHM of the polynomial curve is used to have a first estimate of the potential region for pulsations and the Height-to-Noise ratio is used to evaluate the significance. We found only a marginal detection of pulsation at $\nu = 2040 \pm 282 \mu\text{Hz}$. To confirm the detection, a fit of the power spectrum is performed. It involves describing pulsations with a gaussian envelope and the noise background with two Harvey-like profiles (Harvey 1985) and white noise. Unfortunately, the Bayesian Maximum a Posteriori estimates gives us a significance for pulsations below 1% when compared to a pure noise fit of the spectrum.

Finally, another team analyzed two sets of lightcurves (LC1 and the one with our own aperture) with the A2Z pipeline (Mathur et al. 2010). Briefly, they looked for the mean large frequency spacing by computing the power spectrum of the power spectrum. We then fitted the background with three components: a Harvey law to model the granulation where the slope was fixed to 4, a Gaussian function for the modes and the white noise. After subtracting the background without the Gaussian function, we fitted another Gaussian function to estimate the frequency of the maximum power. A blind run of the A2Z pipeline finds some excess of power around 1000 μHz but no frequency spacing that agrees with the global seismic scaling relations (Kjeldsen & Bedding 1995) is measured with a high level of confidence level. By forcing the pipeline to look around 2000 μHz , a frequency spacing of $\sim 84 \mu\text{Hz}$ is measured with more than 95% confidence level but no Gaussian fit converged to obtain ν_{max} . These results lead to a non detection of the modes with the A2Z pipeline.

6. DISCUSSION

6.1. Impact of magnetic activity on the solar-like oscillations

⁴ <https://github.com/EnricoCorsaro/DIAMONDS>

⁵ <https://github.com/EnricoCorsaro/Background>

We discuss here the analysis of the TESS data and the non-detection of pulsation modes on the solar-like star GJ 504. While some hints of appearance of frequency spacing was found by the application of one of the methods, no reliable detection of solar-like oscillations can finally be reported. It is possible that this might be due to the high noise of the TESS data and the fact that only one sector was available. However, another possible explanation can be attributed to the presence of a high level of magnetic activity. In fact, several authors have already shown that magnetic activity is responsible for suppression of solar-like oscillations as already found in several targets (e.g. [García et al. 2010](#); [Chaplin et al. 2011b](#); [Mathur et al. 2019b](#)). The evolutionary stage, the estimate of the age and the analysis of the magnetic activity indexes of GJ 504 as developed in Sects. 4.2 reveal a level of magnetic activity typical of young solar-like objects (e.g. [Böhm-Vitense 2007](#); [Hall et al. 2007](#)). In fact, the analysis of the chromospheric emission, through the S-index, has highlighted a fairly high level of magnetic activity (mean S-index = 0.313), ~ 1.8 times that of the Sun. The study of the periodicities with the Lomb-Scargle algorithm has pointed out a main principal cycle at 11.97 years, in agreement with the 11.79 ± 0.28 a detected cycle by [Boro Saikia et al. \(2018\)](#), but also revealed the presence of other smaller amplitude cycles. The coexistence of different cycles is a typical characteristic of fast rotating stars, where a higher number of dynamo modes are excited ([Durney et al. 1981](#); [Oláh et al. 2016](#)), as it is the case of this star for which we found $P_{\text{rot}} \simeq 12.5$ days.

Once the stellar rotation and the main activity cycle period are known, we can compute the ratio $P_{\text{cyc}}/P_{\text{rot}}$, a quantity which is known to be related to the dynamo number N_D (see e.g., [Soon et al. 1993](#); [Baliunas et al. 1996](#)). For stars older than 2.5 Gyrs, like the Sun, the quantity $\log(P_{\text{cyc}}/P_{\text{rot}})$ is typically around 2 (see Fig. 6 in [Oláh et al. \(2016\)](#)), while we obtain 2.54. This result indicates that GJ 504 is an active star with an age smaller than the one where the transition from spot to faculae domination, associated with a Rossby number ~ 1 and an age ~ 2.55 Gyr ([Reinhold et al. 2019](#)), is believed to happen. This is in agreement with our age estimation of 1.3 ± 1.3 Gyr. This is also consistent with the fact that [Reinhold et al. \(2019\)](#) found the photometric and chromospheric variability to be out of phase ($\Delta\phi = 0.34$), indicating that the star is still in the spot-dominated activity regime which characterize the young and active stars.

Concerning our attempt to detect solar-like pulsations, we used the calibrated formula by [Bonanno et al. \(2014\)](#), to relate the Mount-Wilson chromospheric S-index to the global oscillation amplitude A_{max} . By using the mean S-index obtained in Sect. 4.2, we obtain for this star a regime of significant oscillation amplitude suppression (see, e.g., Fig. 2 of [Bonanno et al. 2014](#)), defined by an expected global oscillation amplitude of $A_{\text{max}} = 1.6$ ppm, which is rather low as compared to the level of background found in the data. This magnetic activity suppression likely justifies the non-detection of an oscillation power excess in the stellar power spectrum. Even in the case of minimum of activity, corresponding to an S-index of 0.247 (see Sec. 4.2), the expected oscillation amplitude would be 2.6 ppm, which is lower than the average background noise measured in the TESS data estimated to be 6.3 ppm from the background fitting we performed.

In addition, as obtained in Sect. 4.2, the S_{ph} of this star is (1231 ± 7.8) ppm during the TESS observations. Knowing that for the Sun, the average S_{ph} value is 166.1 ppm, we must conclude once more that GJ 504 appears to be very active (7.5 times higher than the Sun) in agreement with the result obtained from the spectroscopic observations. Comparing this level of activity with the stars with and without detection of modes (see Figure 10 of [Mathur et al. 2019a](#)), only 3 stars with a detection of solar-like oscillations have an S_{ph} above 1000 ppm. For these stars, the comparison of the amplitude of the modes observed in the *Kepler* data and the predicted amplitude gives that $A_{\text{max,obs}}/A_{\text{max,pred}} \sim 0.8$ in average, varying between 0.70 and 0.93. This means that we can have a reduction from 7 to 30% in the amplitude of the modes. In the case that we are dominated by the noise, this can even add to the explanation of the non detection of the modes in this star. Note that these three *Kepler* stars are metal poor (with $[\text{Fe}/\text{H}]$ around -0.2dex), which according to [Samadi \(2011\)](#) can lead to higher amplitudes and could counter-balance the effect of the surface magnetic activity.

6.2. Implications of the oscillatory behaviour on the age of GJ 504

In the attempt to better discern the most plausible stellar characteristics able to resemble GJ 504, it is possible to compare the properties of the oscillation frequencies calculated for the produced grid of theoretical models with the average properties, although uncertain, of the observed oscillation spectrum. Among all the calculated models, only Model 2 of Table 3 is able to reproduce within the errors the value of large separation found in Sec 5. We notice that models that reproduce this large separation seem to show values of $\log g$ and T_{eff} which lie nearly at the edges of the one-sigma error box (see Fig. 2).

The predicted oscillatory behaviour can be evinced from plots such as those shown in Figure 8, which reproduce the so called échelle diagrams obtained for Model 1 and Model 2 of Table 3, in which the oscillation frequencies are plotted as a function of the frequency modulo the large separation, and modes of low harmonic degree form roughly vertical ridges. The figures clearly show that models with small differences will show a different pattern of individual frequencies and hence have a well recognizable oscillatory behaviour, if the individual frequencies could have been detected.

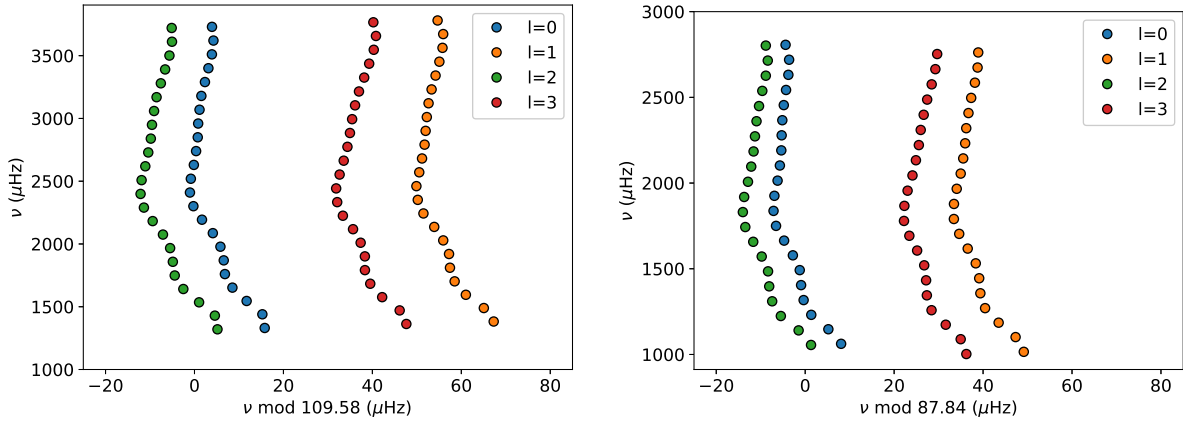


Figure 8. Echelle diagrams calculated for the two selected structure models: Model 1 (left panel) and Model 2 (right panel) of Table 3. Different colours are used to distinguish modes with different harmonic degrees.

Table 4. The parameters of GJ 504 as derived by the present analysis based on the use of TESS and Mount Wilson data.

	Present value
P_{cyc} (a)	11.97
P_{rot} (d)	12.5 ± 2.8
S -index	0.313 ± 0.07
S_{ph} (ppm)	1231 ± 7.8
Age (Gyr)	1.3 ± 1.3
M/M_{\odot}	1.28 ± 0.07
R/R_{\odot}	1.38 ± 0.20
$\Delta\nu$ (μHz)	85 ± 3.6
ν_{max} (μHz)	1919 ± 40

NOTE— P_{cyc} and P_{rot} are the magnetic activity cycle and the surface rotation period respectively. M/M_{\odot} is the mass of the star, R/R_{\odot} is the surface stellar radius, while $\Delta\nu$ and ν_{max} are the dubious values of large separation and frequency of maximum amplitude of oscillation provided by the present analysis .

443 It is very interesting to point out that models that match the SED luminosity, are characterized by a very young age $\leq 0.7\text{Gyr}$,
444 while models which reproduce the provisional large separation 85.0 ± 3.6 show a more evolved structures with age above 2 Gyr
445 and higher luminosity. It is clear that even just the measurement of the large separation, if confirmed, will definitely help to
446 constrain the debated evolutionary state of this target and of its companion. But this will be achieved only with better conditions
447 of signal to noise ratio (i. e., spectroscopic observations, smaller cadence mode etc....).

448

7. CONCLUSION

In this article we present a new attempt to study the solar-like star GJ 504, observed by the space mission TESS and known to host an exoplanet with values of mass and radius not yet confirmed. Unfortunately, we did not succeed to characterize this star by means of asteroseismic techniques, since we did not find evidence for a clear excess of power, although a marginal detection of pulsations seems to manifest at about $\nu_{\max} = 1919 \pm 40 \mu\text{Hz}$ with some indication of large separation with $\Delta\nu = (85 \pm 3.6) \mu\text{Hz}$. This non detection can be explained by the high level of magnetic activity for the star. Indeed the spectroscopic analysis yields an S-index of 0.313 and the photometric analysis of the TESS light curves provides a magnetic proxy S_{ph} of 1231 ppm, both indexes being much larger than the solar value of 0.170 and 161 ppm respectively. Given the values of the S-index and S_{ph} , the modes are predicted to suffer an important decrease of their amplitudes, probably close to the noise level in the TESS observations.

Nevertheless, all the results that we have deduced by analyzing the photometric data by the TESS space mission, supported by the measurements collected by the Mount Wilson Observatory long term campaign spanning nearly 30 years and by the modeling procedures have allowed us to get important conclusions on the large debated parameters of this target. In Table 4 we summarize the stellar parameters that best represent GJ 504.

Firstly, the analysis of the three decades long Mount Wilson spectroscopic observations yields the detection of a main magnetic cycle of 11.97 a and, at least, other two smaller amplitude cycles of 5.75 a and 3.59 a.

Further, the analysis of the Mount Wilson data allowed us to measure a stellar rotational period $P_{\text{rot}} = 12.5$ d, while the TESS light curves show a modulation of 3.4 d. Thus, we are able to conclude that it is very likely that the short length of one TESS sector leads to the measurement of a harmonic of the real rotational period.

The stellar radius and mass have been calculated from stellar models constrained on spectroscopic measurements of gravity, metallicity and effective temperature only. Moreover, the value of the stellar radius results in agreement with independent measurements obtained in the present article by applying the SED and the SBCR methods, but also with the more accurate interferometric radius determined by (Bonnetfoy et al. 2018).

The age of GJ 504, as obtained by stellar modelling based on accurate spectroscopic fundamental parameters, appears to be $\text{Age} \leq 2.6$ Gyr in agreement, within the quoted uncertainties, with previous finding by D’Orazi et al. (2017) and Kuzuhara et al. (2013). In particular, the rotational period and the main magnetic cycle locate this G-type star in the regime of chromospheric activity dominated by the superposition of several magnetic cycles during which, as shown by van Saders et al. (2016) and Metcalfe & van Saders (2017), the magnetic braking is still in act while the rotation is slowing down. This situation put this target well before the magnetic transition, which will bring this star at the age of about 4-5 Gyr to the shutdown of the magnetic braking reaching a low activity state. We would like to point out that the actual scenario is compatible with a standard tidal interaction between the star and its companion and the hypothesis of engulfment of a sub-stellar companion, as previously proposed (Fuhrmann & Chini 2015), is no longer necessary to explain the low rotational period and the age of the star.

Adopting this new age value, along with SPHERE JHK_1K_2 photometry for the companion (Bonnetfoy et al. 2018) and the COND-AMES model atmospheres (Baraffe et al. 2003), we gather companion mass and radius of $M_{\text{p}} = (16.5 \pm 4.8)M_{\text{Jup}}$ and $R_{\text{p}} = (1.00 \pm 0.03)R_{\text{Jup}}$ (the related errors are simply the standard deviation from the four photometric bands, so they are certainly under-estimated). Hence, given the large uncertainty in age, we cannot confirm/disprove from the present study whether GJ 504b is located in the brown dwarf or planetary regime.

A substantial step forward in the characterization of this star will be obtained by scheduled TESS observations during Sector 50 with 20-second cadence mode. The improved precision, according to our calculations, will allow to detect oscillations and to better constrain the parameters of this star and of its companion by means of asteroseismic techniques. In fact, observations of this target with a 20-second cadence might reduce the level of noise as shown for instance by Huber et al. (2022) and therefore increase the chance of detecting the oscillation power excess. Based on TESS magnitude of 4.6552 ± 0.0073 (Stassun et al. 2019) the 20-second cadence data should yield an improvement in photometric precision of $\approx 30\%$ due to the reduced influence of pointing jitter on cosmic-ray rejection for bright stars (Huber et al. 2022). Furthermore, the measured period $P_{\text{cyc}} \approx 12$ a of the main magnetic cycle implies that the next stellar magnetic minimum should occur between 2022 and 2023, overlapping with TESS Sector 50, which would minimize the amplitude-suppressing effect of magnetic activity.

For the future, we believe that GJ 504 might represent an ideal target also for the ESA/PLATO (Rauer et al. 2016) space mission, with scheduled launch in the end of 2026, having the potential with its high-precision, high-time-resolution and high-duty-cycle photometry to detect individual oscillation frequencies in this star, leading finally not only to clarify the evolutionary state of this system but also to solve hot questions related to the use of rotation and magnetic activity as a diagnostic of stellar age and finally leading to a clear and more accurate concept of gyrochronology.

498 The publication of the present article has been supported by INAF through the Main-Stream call 2018-‘Stellar evolution and
 499 pulsations in the context of the PLATO space mission’. This paper includes data collected with the TESS mission, obtained
 500 from the MAST data archive at the Space Telescope Science Institute (STScI). Funding for the TESS mission is provided by
 501 the NASA Explorer Program. STScI is operated by the Association of Universities for Research in Astronomy, Inc., under
 502 NASA contract NAS 5–26555. R.A.G. Acknowledges funding from the PLATO CNES grant. S.M. acknowledges support by the
 503 Spanish Ministry of Science and Innovation with the Ramon y Cajal fellowship number RYC-2015-17697 and the grant number
 504 PID2019-107187GB-I00. D.B. acknowledges support from the National Aeronautics and Space Administration under the Living
 505 With A Star program, grant number NNX16AB76G. R.R. is a PhD student of the PhD course in Astronomy, Astrophysics and
 506 Space Science, a joint research program between the University of Rome “Tor Vergata”, the Sapienza University of Rome and
 507 the National Institute of Astrophysics (INAF).

REFERENCES

- 508 Addison, B. C., Wright, D. J., Nicholson, B. A., et al. 2021,
 509 MNRAS, 502, 3704, doi: [10.1093/mnras/staa3960](https://doi.org/10.1093/mnras/staa3960)
- 510 Angulo, C., Arnould, M., Rayet, M., et al. 1999, NuPhA, 656, 3,
 511 doi: [10.1016/S0375-9474\(99\)00030-5](https://doi.org/10.1016/S0375-9474(99)00030-5)
- 512 Baglin, A., Auvergne, M., Boisnard, L., et al. 2006, in 36th
 513 COSPAR Scientific Assembly, Vol. 36, 3749
- 514 Baliunas, S. L., Nesme-Ribes, E., Sokoloff, D., & Soon, W. H.
 515 1996, ApJ, 460, 848, doi: [10.1086/177014](https://doi.org/10.1086/177014)
- 516 Baliunas, S. L., Donahue, R. A., Soon, W. H., et al. 1995, ApJ,
 517 438, 269, doi: [10.1086/175072](https://doi.org/10.1086/175072)
- 518 Baraffe, I., Chabrier, G., Barman, T. S., Allard, F., & Hauschildt,
 519 P. H. 2003, A&A, 402, 701, doi: [10.1051/0004-6361:20030252](https://doi.org/10.1051/0004-6361:20030252)
- 520 Barnes, S. A. 2007, ApJ, 669, 1167, doi: [10.1086/519295](https://doi.org/10.1086/519295)
- 521 Battistini, C., & Bensby, T. 2015, A&A, 577, A9,
 522 doi: [10.1051/0004-6361/201425327](https://doi.org/10.1051/0004-6361/201425327)
- 523 Beck, P. G., Montalbán, J., Kallinger, T., et al. 2012, Nature, 481,
 524 55, doi: [10.1038/nature10612](https://doi.org/10.1038/nature10612)
- 525 Bedding, T. R. 2014, in Asteroseismology, ed. P. L. Pallé &
 526 C. Esteban, 60
- 527 Bedding, T. R., & Kjeldsen, H. 2003, PASA, 20, 203,
 528 doi: [10.1071/AS03025](https://doi.org/10.1071/AS03025)
- 529 Bedding, T. R., Mosser, B., Huber, D., et al. 2011, Nature, 471,
 530 608, doi: [10.1038/nature09935](https://doi.org/10.1038/nature09935)
- 531 Belkacem, K., Goupil, M. J., Dupret, M. A., et al. 2011, A&A,
 532 530, A142, doi: [10.1051/0004-6361/201116490](https://doi.org/10.1051/0004-6361/201116490)
- 533 Benomar, O., Baudin, F., Chaplin, W., Elsworth, Y., &
 534 Appourchaux, T. 2012, \mnras, 420, 2178,
 535 doi: [10.1111/j.1365-2966.2011.20184.x](https://doi.org/10.1111/j.1365-2966.2011.20184.x)
- 536 Böhm-Vitense, E. 1958, ZA, 46, 108
- 537 —. 2007, ApJ, 657, 486, doi: [10.1086/510482](https://doi.org/10.1086/510482)
- 538 Bonanno, A., Corsaro, E., & Karoff, C. 2014, A&A, 571, A35,
 539 doi: [10.1051/0004-6361/201424632](https://doi.org/10.1051/0004-6361/201424632)
- 540 Bonnefoy, M., Perraut, K., Lagrange, A. M., et al. 2018, A&A,
 541 618, A63, doi: [10.1051/0004-6361/201832942](https://doi.org/10.1051/0004-6361/201832942)
- 542 Boro Saikia, S., Marvin, C. J., Jeffers, S. V., et al. 2018, A&A, 616,
 543 A108, doi: [10.1051/0004-6361/201629518](https://doi.org/10.1051/0004-6361/201629518)
- 544 Borucki, W. J., Koch, D., Basri, G., et al. 2010, Science, 327, 977,
 545 doi: [10.1126/science.1185402](https://doi.org/10.1126/science.1185402)
- 546 Borucki, W. J., Agol, E., Fressin, F., et al. 2013, Science, 340, 587,
 547 doi: [10.1126/science.1234702](https://doi.org/10.1126/science.1234702)
- 548 Brown, T. M., Gilliland, R. L., Noyes, R. W., & Ramsey, L. W.
 549 1991, ApJ, 368, 599, doi: [10.1086/169725](https://doi.org/10.1086/169725)
- 550 Buzasi, Derek, L., Carboneau, L., Hessler, C., Lezcano, A., &
 551 Preston, H. 2016, IAU Focus Meeting, 29B, 673,
 552 doi: [10.1017/S1743921316006335](https://doi.org/10.1017/S1743921316006335)
- 553 Campante, T. L., Schofield, M., Kuszlewicz, J. S., et al. 2016, ApJ,
 554 830, 138, doi: [10.3847/0004-637X/830/2/138](https://doi.org/10.3847/0004-637X/830/2/138)
- 555 Capitanio, L., Lallement, R., Vergely, J. L., Elyajouri, M., &
 556 Monreal-Ibero, A. 2017, A&A, 606, A65,
 557 doi: [10.1051/0004-6361/201730831](https://doi.org/10.1051/0004-6361/201730831)
- 558 Ceillier, T., van Saders, J., García, R. A., et al. 2016, MNRAS,
 559 456, 119, doi: [10.1093/mnras/stv2622](https://doi.org/10.1093/mnras/stv2622)
- 560 Chaplin, W. J., Houdek, G., Appourchaux, T., et al. 2008, A&A,
 561 485, 813, doi: [10.1051/0004-6361:200809695](https://doi.org/10.1051/0004-6361:200809695)
- 562 Chaplin, W. J., Kjeldsen, H., Bedding, T. R., et al. 2011a, ApJ, 732,
 563 54, doi: [10.1088/0004-637X/732/1/54](https://doi.org/10.1088/0004-637X/732/1/54)
- 564 Chaplin, W. J., Bedding, T. R., Bonanno, A., et al. 2011b, ApJL,
 565 732, L5, doi: [10.1088/2041-8205/732/1/L5](https://doi.org/10.1088/2041-8205/732/1/L5)
- 566 Chaplin, W. J., Sanchis-Ojeda, R., Campante, T. L., et al. 2013,
 567 ApJ, 766, 101, doi: [10.1088/0004-637X/766/2/101](https://doi.org/10.1088/0004-637X/766/2/101)
- 568 Chontos, A., Huber, D., Kjeldsen, H., et al. 2020, arXiv e-prints,
 569 arXiv:2012.10797. <https://arxiv.org/abs/2012.10797>
- 570 Christensen-Dalsgaard, J. 1988, in Advances in Helio- and
 571 Asteroseismology, ed. J. Christensen-Dalsgaard & S. Frandsen,
 572 Vol. 123, 295
- 573 Christensen-Dalsgaard, J. 2008a, Ap&SS, 316, 13,
 574 doi: [10.1007/s10509-007-9675-5](https://doi.org/10.1007/s10509-007-9675-5)
- 575 —. 2008b, Ap&SS, 316, 113, doi: [10.1007/s10509-007-9689-z](https://doi.org/10.1007/s10509-007-9689-z)
- 576 Corsaro, E., & De Ridder, J. 2014, A&A, 571, A71,
 577 doi: [10.1051/0004-6361/201424181](https://doi.org/10.1051/0004-6361/201424181)
- 578 Corsaro, E., Mathur, S., García, R. A., et al. 2017, A&A, 605, A3,
 579 doi: [10.1051/0004-6361/201731094](https://doi.org/10.1051/0004-6361/201731094)

- 580 Cutri, R. M., Skrutskie, M. F., van Dyk, S., et al. 2003, *VizieR*
581 *Online Data Catalog*, II/246
- 582 da Silva, R., Porto de Mello, G. F., Milone, A. C., et al. 2012,
583 *A&A*, 542, A84, doi: [10.1051/0004-6361/201118751](https://doi.org/10.1051/0004-6361/201118751)
- 584 Di Mauro, M. P. 2016, in *Frontier Research in Astrophysics II*
585 (FRAPWS2016), 29. <https://arxiv.org/abs/1703.07604>
- 586 Di Mauro, M. P., Christensen-Dalsgaard, J., Paternò, L., &
587 D’Antona, F. 2004, *SoPh*, 220, 185,
588 doi: [10.1023/B:SOLA.0000031379.44874.3e](https://doi.org/10.1023/B:SOLA.0000031379.44874.3e)
- 589 Donahue, R. A., Saar, S. H., & Baliunas, S. L. 1996, *ApJ*, 466,
590 384, doi: [10.1086/177517](https://doi.org/10.1086/177517)
- 591 D’Orazi, V., Desidera, S., Gratton, R. G., et al. 2017, *A&A*, 598,
592 A19, doi: [10.1051/0004-6361/201629283](https://doi.org/10.1051/0004-6361/201629283)
- 593 Durney, B. R., Mihalas, D., & Robinson, R. D. 1981, *PASP*, 93,
594 537, doi: [10.1086/130878](https://doi.org/10.1086/130878)
- 595 Egeland, R., Soon, W., Baliunas, S., et al. 2017, *ApJ*, 835, 25,
596 doi: [10.3847/1538-4357/835/1/25](https://doi.org/10.3847/1538-4357/835/1/25)
- 597 Fabbian, D., Simoniello, R., Collet, R., et al. 2017, *Astronomische*
598 *Nachrichten*, 338, 753, doi: [10.1002/asna.201713403](https://doi.org/10.1002/asna.201713403)
- 599 Fuhrmann, K. 2004, *Astronomische Nachrichten*, 325, 3,
600 doi: [10.1002/asna.200310173](https://doi.org/10.1002/asna.200310173)
- 601 Fuhrmann, K., & Chini, R. 2015, *ApJ*, 806, 163,
602 doi: [10.1088/0004-637X/806/2/163](https://doi.org/10.1088/0004-637X/806/2/163)
- 603 Gaia Collaboration. 2018, *VizieR Online Data Catalog*, I/345
604 —. 2020, *VizieR Online Data Catalog*, I/350
- 605 Gandolfi, D., Barragán, O., Livingston, J. H., et al. 2018, *A&A*,
606 619, L10, doi: [10.1051/0004-6361/201834289](https://doi.org/10.1051/0004-6361/201834289)
- 607 García, R. A., & Ballot, J. 2019, *Living Reviews in Solar Physics*,
608 16, 4, doi: [10.1007/s41116-019-0020-1](https://doi.org/10.1007/s41116-019-0020-1)
- 609 García, R. A., Mathur, S., Salabert, D., et al. 2010, *Science*, 329,
610 1032, doi: [10.1126/science.1191064](https://doi.org/10.1126/science.1191064)
- 611 García, R. A., Hekker, S., Stello, D., et al. 2011, *MNRAS*, 414, L6,
612 doi: [10.1111/j.1745-3933.2011.01042.x](https://doi.org/10.1111/j.1745-3933.2011.01042.x)
- 613 García, R. A., Mathur, S., Pires, S., et al. 2014a, *A&A*, 568, A10,
614 doi: [10.1051/0004-6361/201323326](https://doi.org/10.1051/0004-6361/201323326)
- 615 García, R. A., Ceillier, T., Salabert, D., et al. 2014b, *A&A*, 572,
616 A34, doi: [10.1051/0004-6361/201423888](https://doi.org/10.1051/0004-6361/201423888)
- 617 Gaulme, P., Jackiewicz, J., Spada, F., et al. 2020, *A&A*, 639, A63,
618 doi: [10.1051/0004-6361/202037781](https://doi.org/10.1051/0004-6361/202037781)
- 619 Gondoin, P. 2018, *A&A*, 616, A154,
620 doi: [10.1051/0004-6361/201731541](https://doi.org/10.1051/0004-6361/201731541)
- 621 Grevesse, N., & Noels, A. 1993, in *Origin and Evolution of the*
622 *Elements*, ed. N. Prantzos, E. Vangioni-Flam, & M. Casse,
623 15–25
- 624 Hall, J. C. 2008, *Living Reviews in Solar Physics*, 5, 2,
625 doi: [10.12942/lrsp-2008-2](https://doi.org/10.12942/lrsp-2008-2)
- 626 Hall, J. C., Lockwood, G. W., & Skiff, B. A. 2007, *AJ*, 133, 862,
627 doi: [10.1086/510356](https://doi.org/10.1086/510356)
- 628 Harvey, J. 1985, *ESA SP*, 235, 199
- 629 Huber, D., Bedding, T. R., Stello, D., et al. 2011, *ApJ*, 743, 143,
630 doi: [10.1088/0004-637X/743/2/143](https://doi.org/10.1088/0004-637X/743/2/143)
- 631 Huber, D., Chaplin, W. J., Christensen-Dalsgaard, J., et al. 2013,
632 *ApJ*, 767, 127, doi: [10.1088/0004-637X/767/2/127](https://doi.org/10.1088/0004-637X/767/2/127)
- 633 Huber, D., Chaplin, W. J., Chontos, A., et al. 2019, *AJ*, 157, 245,
634 doi: [10.3847/1538-3881/ab1488](https://doi.org/10.3847/1538-3881/ab1488)
- 635 Huber, D., White, T. R., Metcalfe, T. S., et al. 2021, *arXiv e-prints*,
636 arXiv:2108.09109. <https://arxiv.org/abs/2108.09109>
- 637 —. 2022, *AJ*, 163, 79, doi: [10.3847/1538-3881/ac3000](https://doi.org/10.3847/1538-3881/ac3000)
- 638 Iglesias, C. A., & Rogers, F. J. 1996, *ApJ*, 464, 943,
639 doi: [10.1086/177381](https://doi.org/10.1086/177381)
- 640 Janson, M., Brandt, T. D., Kuzuhara, M., et al. 2013, *ApJL*, 778,
641 L4, doi: [10.1088/2041-8205/778/1/L4](https://doi.org/10.1088/2041-8205/778/1/L4)
- 642 Jenkins, J. M., Twicken, J. D., McCauliff, S., et al. 2016, in *Society*
643 *of Photo-Optical Instrumentation Engineers (SPIE) Conference*
644 *Series*, Vol. 9913, *Software and Cyberinfrastructure for*
645 *Astronomy IV*, ed. G. Chiozzi & J. C. Guzman, 99133E,
646 doi: [10.1117/12.2233418](https://doi.org/10.1117/12.2233418)
- 647 Jones, E., Oliphant, T., Peterson, P., et al. 2001, *SciPy: Open*
648 *source scientific tools for Python*. <http://www.scipy.org/>
- 649 Kiefer, R., Schad, A., Davies, G., & Roth, M. 2017, *A&A*, 598,
650 A77, doi: [10.1051/0004-6361/201628469](https://doi.org/10.1051/0004-6361/201628469)
- 651 Kjeldsen, H., & Bedding, T. R. 1995, *A&A*, 293, 87.
652 <https://arxiv.org/abs/astro-ph/9403015>
- 653 Kjeldsen, H., Bedding, T. R., Arentoft, T., et al. 2008, *ApJ*, 682,
654 1370, doi: [10.1086/589142](https://doi.org/10.1086/589142)
- 655 Kuzuhara, M., Tamura, M., Kudo, T., et al. 2013, *ApJ*, 774, 11,
656 doi: [10.1088/0004-637X/774/1/11](https://doi.org/10.1088/0004-637X/774/1/11)
- 657 Lallement, R., Vergely, J. L., Valette, B., et al. 2014, *A&A*, 561,
658 A91, doi: [10.1051/0004-6361/201322032](https://doi.org/10.1051/0004-6361/201322032)
- 659 Lebreton, Y., & Goupil, M. J. 2014, *A&A*, 569, A21,
660 doi: [10.1051/0004-6361/201423797](https://doi.org/10.1051/0004-6361/201423797)
- 661 Lebreton, Y., Goupil, M. J., & Montalbán, J. 2014, in *EAS*
662 *Publications Series*, Vol. 65, *EAS Publications Series*, 177–223,
663 doi: [10.1051/eas/1465005](https://doi.org/10.1051/eas/1465005)
- 664 Li, T. D., Bi, S. L., Chen, Y. Q., et al. 2012, *ApJ*, 746, 143,
665 doi: [10.1088/0004-637X/746/2/143](https://doi.org/10.1088/0004-637X/746/2/143)
- 666 Lomb, N. R. 1976, *Ap&SS*, 39, 447, doi: [10.1007/BF00648343](https://doi.org/10.1007/BF00648343)
- 667 Maldonado, J., Eiroa, C., Villaver, E., Montesinos, B., & Mora, A.
668 2015, *A&A*, 579, A20, doi: [10.1051/0004-6361/201525764](https://doi.org/10.1051/0004-6361/201525764)
- 669 Mamajek, E. E., & Hillenbrand, L. A. 2008, *ApJ*, 687, 1264,
670 doi: [10.1086/591785](https://doi.org/10.1086/591785)
- 671 Mathur, S., García, R. A., Bugnet, L., et al. 2019a, *Frontiers in*
672 *Astronomy and Space Sciences*, 6, 46,
673 doi: [10.3389/fspas.2019.00046](https://doi.org/10.3389/fspas.2019.00046)
- 674 —. 2019b, *Frontiers in Astronomy and Space Sciences*, 6, 46,
675 doi: [10.3389/fspas.2019.00046](https://doi.org/10.3389/fspas.2019.00046)
- 676 Mathur, S., Salabert, D., García, R. A., & Ceillier, T. 2014a,
677 *Journal of Space Weather and Space Climate*, 4, A15,
678 doi: [10.1051/swsc/2014011](https://doi.org/10.1051/swsc/2014011)

- 679 Mathur, S., García, R. A., Régulo, C., et al. 2010, *A&A*, 511, A46,
680 doi: [10.1051/0004-6361/200913266](https://doi.org/10.1051/0004-6361/200913266)
- 681 Mathur, S., García, R. A., Ballot, J., et al. 2014b, *A&A*, 562, A124,
682 doi: [10.1051/0004-6361/201322707](https://doi.org/10.1051/0004-6361/201322707)
- 683 McQuillan, A., Mazeh, T., & Aigrain, S. 2014, *ApJS*, 211, 24,
684 doi: [10.1088/0067-0049/211/2/24](https://doi.org/10.1088/0067-0049/211/2/24)
- 685 Mermilliod, J. C. 2006, *VizieR Online Data Catalog*, II/168
- 686 Messina, S., Pizzolato, N., Guinan, E. F., & Rodonò, M. 2003,
687 *A&A*, 410, 671, doi: [10.1051/0004-6361:20031203](https://doi.org/10.1051/0004-6361:20031203)
- 688 Metcalfe, T. S., & van Saders, J. 2017, *SoPh*, 292, 126,
689 doi: [10.1007/s11207-017-1157-5](https://doi.org/10.1007/s11207-017-1157-5)
- 690 Metcalfe, T. S., Monteiro, M. J. P. F. G., Thompson, M. J., et al.
691 2010, *ApJ*, 723, 1583, doi: [10.1088/0004-637X/723/2/1583](https://doi.org/10.1088/0004-637X/723/2/1583)
- 692 Metcalfe, T. S., van Saders, J. L., Basu, S., et al. 2020, *ApJ*, 900,
693 154, doi: [10.3847/1538-4357/aba963](https://doi.org/10.3847/1538-4357/aba963)
- 694 —. 2021, *ApJ*, 921, 122, doi: [10.3847/1538-4357/ac1f19](https://doi.org/10.3847/1538-4357/ac1f19)
- 695 Mishenina, T. V., Pignatari, M., Korotin, S. A., et al. 2013, *A&A*,
696 552, A128, doi: [10.1051/0004-6361/201220687](https://doi.org/10.1051/0004-6361/201220687)
- 697 Müllner, M., Zwintz, K., Corsaro, E., et al. 2021, *A&A*, 647,
698 A168, doi: [10.1051/0004-6361/202039578](https://doi.org/10.1051/0004-6361/202039578)
- 699 Nielsen, M. B., Ball, W. H., Standing, M. R., et al. 2020, *arXiv*
700 e-prints, arXiv:2007.00497
- 701 Nishiyama, S., Tamura, M., Hatano, H., et al. 2009, *ApJ*, 696,
702 1407, doi: [10.1088/0004-637X/696/2/1407](https://doi.org/10.1088/0004-637X/696/2/1407)
- 703 Oetjens, A., Carone, L., Bergemann, M., & Serenelli, A. 2020,
704 *A&A*, 643, A34, doi: [10.1051/0004-6361/202038653](https://doi.org/10.1051/0004-6361/202038653)
- 705 Oláh, K., Kővári, Z., Petrovay, K., et al. 2016, *A&A*, 590, A133,
706 doi: [10.1051/0004-6361/201628479](https://doi.org/10.1051/0004-6361/201628479)
- 707 Paunzen, E. 2015, *VizieR Online Data Catalog*, J/A+A/580/A23
- 708 Pires, S., Mathur, S., García, R. A., et al. 2015, *A&A*, 574, A18,
709 doi: [10.1051/0004-6361/201322361](https://doi.org/10.1051/0004-6361/201322361)
- 710 Pont, F., & Eyer, L. 2004, *MNRAS*, 351, 487,
711 doi: [10.1111/j.1365-2966.2004.07780.x](https://doi.org/10.1111/j.1365-2966.2004.07780.x)
- 712 Radick, R. R., Lockwood, G. W., Skiff, B. A., & Baliunas, S. L.
713 1998, *ApJS*, 118, 239, doi: [10.1086/313135](https://doi.org/10.1086/313135)
- 714 Ramírez, I., Allende Prieto, C., & Lambert, D. L. 2013, *ApJ*, 764,
715 78, doi: [10.1088/0004-637X/764/1/78](https://doi.org/10.1088/0004-637X/764/1/78)
- 716 Rauer, H., Aerts, C., Cabrera, J., & PLATO Team. 2016,
717 *Astronomische Nachrichten*, 337, 961,
718 doi: [10.1002/asna.201612408](https://doi.org/10.1002/asna.201612408)
- 719 Reinhold, T., Bell, K. J., Kuszlewicz, J., Hekker, S., & Shapiro,
720 A. I. 2019, *A&A*, 621, A21, doi: [10.1051/0004-6361/201833754](https://doi.org/10.1051/0004-6361/201833754)
- 721 Ricker, G. R., Winn, J. N., Vanderspek, R., et al. 2014, in *Society*
722 *of Photo-Optical Instrumentation Engineers (SPIE) Conference*
723 *Series*, Vol. 9143, *Space Telescopes and Instrumentation 2014:*
724 *Optical, Infrared, and Millimeter Wave*, ed. J. Oschmann,
725 Jacobus M., M. Clampin, G. G. Fazio, & H. A. MacEwen,
726 914320, doi: [10.1117/12.2063489](https://doi.org/10.1117/12.2063489)
- 727 Rogers, F. J., & Nayfonov, A. 2002, *ApJ*, 576, 1064,
728 doi: [10.1086/341894](https://doi.org/10.1086/341894)
- 729 Salsi, A., Nardetto, N., Mourard, D., et al. 2021, *A&A*, 652, A26,
730 doi: [10.1051/0004-6361/202140763](https://doi.org/10.1051/0004-6361/202140763)
- 731 Samadi, R. 2011, *Stochastic Excitation of Acoustic Modes in*
732 *Stars*, ed. J.-P. Rozelot & C. Neiner, Vol. 832, 305,
733 doi: [10.1007/978-3-642-19928-8_11](https://doi.org/10.1007/978-3-642-19928-8_11)
- 734 Santos, A. R. G., Breton, S. N., Mathur, S., & García, R. A. 2021,
735 *ApJS*, 255, 17, doi: [10.3847/1538-4365/ac033f](https://doi.org/10.3847/1538-4365/ac033f)
- 736 Santos, A. R. G., García, R. A., Mathur, S., et al. 2019, *ApJS*, 244,
737 21, doi: [10.3847/1538-4365/ab3b56](https://doi.org/10.3847/1538-4365/ab3b56)
- 738 Santos, A. R. G., Campante, T. L., Chaplin, W. J., et al. 2018,
739 *ApJS*, 237, 17, doi: [10.3847/1538-4365/aac9b6](https://doi.org/10.3847/1538-4365/aac9b6)
- 740 Scargle, J. D. 1982, *ApJ*, 263, 835, doi: [10.1086/160554](https://doi.org/10.1086/160554)
- 741 Schofield, M., Chaplin, W. J., Huber, D., et al. 2019, *ApJS*, 241,
742 12, doi: [10.3847/1538-4365/ab04f5](https://doi.org/10.3847/1538-4365/ab04f5)
- 743 Silva Aguirre, V., Davies, G. R., Basu, S., et al. 2015, *MNRAS*,
744 452, 2127, doi: [10.1093/mnras/stv1388](https://doi.org/10.1093/mnras/stv1388)
- 745 Skemer, A. J., Morley, C. V., Zimmerman, N. T., et al. 2016, *ApJ*,
746 817, 166, doi: [10.3847/0004-637X/817/2/166](https://doi.org/10.3847/0004-637X/817/2/166)
- 747 Skumanich, A. 1972, *ApJ*, 171, 565, doi: [10.1086/151310](https://doi.org/10.1086/151310)
- 748 Soderblom, D. R., Hillenbrand, L. A., Jeffries, R. D., Mamajek,
749 E. E., & Naylor, T. 2014, in *Protostars and Planets VI*, ed.
750 H. Beuther, R. S. Klessen, C. P. Dullemond, & T. Henning, 219,
751 doi: [10.2458/azu_uapress_9780816531240-ch010](https://doi.org/10.2458/azu_uapress_9780816531240-ch010)
- 752 Soon, W. H., Baliunas, S. L., & Zhang, Q. 1993, *ApJL*, 414, L33,
753 doi: [10.1086/186989](https://doi.org/10.1086/186989)
- 754 Stassun, K. G., Collins, K. A., & Gaudi, B. S. 2017, *AJ*, 153, 136,
755 doi: [10.3847/1538-3881/aa5df3](https://doi.org/10.3847/1538-3881/aa5df3)
- 756 Stassun, K. G., Corsaro, E., Pepper, J. A., & Gaudi, B. S. 2018, *AJ*,
757 155, 22, doi: [10.3847/1538-3881/aa998a](https://doi.org/10.3847/1538-3881/aa998a)
- 758 Stassun, K. G., & Torres, G. 2016, *AJ*, 152, 180,
759 doi: [10.3847/0004-6256/152/6/180](https://doi.org/10.3847/0004-6256/152/6/180)
- 760 —. 2021, *ApJL*, 907, L33, doi: [10.3847/2041-8213/abdaad](https://doi.org/10.3847/2041-8213/abdaad)
- 761 Stassun, K. G., Oelkers, R. J., Paegert, M., et al. 2019, *AJ*, 158,
762 138, doi: [10.3847/1538-3881/ab3467](https://doi.org/10.3847/1538-3881/ab3467)
- 763 Stello, D., Bruntt, H., Preston, H., & Buzasi, D. 2008, *The*
764 *Astrophysical Journal*, 674, L53, doi: [10.1086/528936](https://doi.org/10.1086/528936)
- 765 Stello, D., Cantiello, M., Fuller, J., et al. 2016, *Nature*, 529, 364,
766 doi: [10.1038/nature16171](https://doi.org/10.1038/nature16171)
- 767 Tassoul, M. 1980, *ApJS*, 43, 469, doi: [10.1086/190678](https://doi.org/10.1086/190678)
- 768 Torrence, C., & Compo, G. P. 1998, *Bulletin of the American*
769 *Meteorological Society*, 79, 61,
770 doi: [10.1175/1520-0477\(1998\)079](https://doi.org/10.1175/1520-0477(1998)079)
- 771 Torres, G., Andersen, J., & Giménez, A. 2010, *A&A Rv*, 18, 67,
772 doi: [10.1007/s00159-009-0025-1](https://doi.org/10.1007/s00159-009-0025-1)
- 773 Valenti, J. A., & Fischer, D. A. 2005, *ApJS*, 159, 141,
774 doi: [10.1086/430500](https://doi.org/10.1086/430500)
- 775 Van Eylen, V., Lund, M. N., Silva Aguirre, V., et al. 2014, *ApJ*,
776 782, 14, doi: [10.1088/0004-637X/782/1/14](https://doi.org/10.1088/0004-637X/782/1/14)
- 777 van Saders, J. L., Ceillier, T., Metcalfe, T. S., et al. 2016, *Nature*,
778 529, 181, doi: [10.1038/nature16168](https://doi.org/10.1038/nature16168)

- 779 Vaughan, A. H., Preston, G. W., & Wilson, O. C. 1978, *PASP*, 90,
780 267, doi: [10.1086/130324](https://doi.org/10.1086/130324)
- 781 Wilson, O. C. 1968, *ApJ*, 153, 221, doi: [10.1086/149652](https://doi.org/10.1086/149652)
- 782 —. 1978, *ApJ*, 226, 379, doi: [10.1086/156618](https://doi.org/10.1086/156618)
- 783 Wright, D. J., Chené, A.-N., De Cat, P., et al. 2011, *ApJL*, 728,
784 L20, doi: [10.1088/2041-8205/728/1/L20](https://doi.org/10.1088/2041-8205/728/1/L20)